Noniterative approach to the missing data problem in coherent diffraction imaging by phase retrieval

Nobuharu Nakajima

Faculty of Engineering, Shizuoka University, 3-5-1 Johoku, Naka-ku, Hamamatsu,

432-8561, Japan

Abstract

When a very intense beam is used for illuminating an object in coherent x-ray diffraction imaging, the intensities at the center of the diffraction pattern for the object are cut off by a beam stop that is utilized to block the intense beam. Until now, only iterative phase-retrieval methods have been applied to the object reconstruction from a single diffraction pattern with a deficiency of central data due to a beam stop. As an alternative method, we here present a noniterative solution, in which an interpolation method based on the sampling theorem for the missing data is used for the object reconstruction with our previously proposed phase-retrieval method using an aperture-array filter. Computer simulations demonstrate the reconstruction of a complex-amplitude object from a single diffraction pattern with a missing data area, which is generally difficult to treat with the iterative methods because a nonnegativity constraint cannot be used for such an object.

OCIS codes: *100.0100 Image processing, 100.5070 Phase retrieval*

1. INTRODUCTION

Lensless coherent x-ray imaging from the diffraction intensity of an object has attracted considerable attention in the past decade since x-rays of coherent and brightness beams had become available from synchrotron radiation sources. In particular, the coherent x-ray imaging has been applied to the reconstruction of a noncrystalline specimen [1-4] or a small crystal [5,6] from its diffraction intensities with a spatial resolution from several to a few tens of nanometers. When such an isolated object is illuminated with a coherent and intense beam, the central intensities of the diffraction pattern of the object are mixed with the direct beam. In this case, there exists the missing data problem for the measurement of the diffraction intensity, because the central intensities of the diffraction pattern are lost by a beam stop used for blocking the intense direct beam. Since the central intensities of the diffraction pattern include the information of the lower spatial frequency of the object structure, the lack of that information makes the object reconstruction difficult and every so often impossible. The conventional approach in the field of diffraction imaging is to replace the missing data in the diffraction pattern by the corresponding spatial frequency calculated from the low-resolution image of an x-ray or electron microscope [7]. This approach, however, makes it impossible to perform the investigation of the dynamics of object structures, and also causes artifacts in the object reconstruction owing to the combination of the different contrast data between the coherent diffraction imaging and the microscopy. Therefore it is desirable to be able to reconstruct an object directly from a single diffraction pattern with missing data.

Until now, a numerical solution to the problem of the object reconstruction from the diffraction pattern with the missing data area has been shown by using only the iterative phase-retrieval method [8]. The three-dimensional structure of a positive object has been reconstructed

[8] from diffraction patterns at different angles by using the iterative method with the nonnegativity constraint, when the missing data are confined within a central speckle size that is proportional to the inverse of the object's extent. However, the reconstruction by iterative methods is accompanied by convergence problems, and hence the methods sometimes stagnate in a local minimum solution different from a true one. In the case of the reconstruction of complex-amplitude objects, the convergence of iterative methods becomes generally even more difficult [9,10], because the nonnegativity constraint that helps convergence in iterative methods cannot be used. Although a nonnegativity constraint on the imaginary part of some complex-amplitude objects has been used [11] to retrieve the phase from the Fourier intensity distribution with a beam stop, such a constraint cannot be applied to generally complex-amplitude objects.

To the best of my knowledge, there is not any noniterative solution to the object reconstruction from a diffraction patter with a deficiency of central data so far. We have recently proposed a noniterative phase-retrieval method using an aperture-array filter to reconstruct a complex-amplitude object from a single diffraction pattern [12]. In this paper we present a noniterative solution to the missing data problem in coherent diffraction imaging, in which an interpolation method based on the sampling theorem [13] is applied to the missing data problem for the object reconstruction by the noniterative phase-retrieval method [12]. It is demonstrated in computer simulations that the present method can cope with the reconstruction of a complex-amplitude object from a single diffraction pattern with missing data due to a beam stop, which is generally difficult to be reconstructed by iterative phase-retrieval methods.

In computer simulations, we demonstrate that, even if the maximum modulus of an illuminating Gaussian beam is ten thousand times larger than the maximum one of a complex-amplitude object, the object can be reliably reconstructed from a single far-field diffraction

pattern with missing data by the use of the present method, provided that the extent of the Gaussian beam is at least four times larger than that of the object and the size of a beam stop covers at most the spatial frequency area within the bounds of the inverse of the object's extent. In other words, almost all energy of the direct Gaussian beam at the far-field plane can be blocked by the beam stop's size, and then the object can be reconstructed by the noniterative phase-retrieval method from diffraction intensity data, of which the missing data are recovered from the diffraction intensities outside the area of the beam stop by using the interpolation method.

In Section 2, we first present a short review of the phase retrieval method using an aperture-array filter, and then develop the procedure to estimate the missing data of two-dimensional (2-D) diffraction intensity by using a one-dimensional (1-D) interpolation method based on the sampling theorem. Such a 1-D interpolation is not so time-consuming as a 2-D one, and is suitable for the present phase-retrieval method based on 1-D calculations. In Section 3, the validity of the present method is demonstrated with computer simulations of the reconstruction of a complex-amplitude object, and we investigate the allowable range of the error for a parameter required for the calculation of the interpolation method (i.e., the error for an extent of the autocorrelation function of the object). In addition, the condition of the missing data size in the present method is compared with that in the iterative method [8]. Concluding remarks are given in Section 4.

2. Interpolation procedure for missing intensities

A. Review of the Phase Retrieval Method Using an Aperture-array Filter

In this paper we apply an interpolation method based on the sampling theorem to the missing data problem for the object reconstruction by the noniterative phase retrieval method using an aperture-array filter [12]. Thus a brief review of the phase retrieval method is described here. Figure 1 shows a schematic of the phase retrieval method. When an object is illuminated by a coherent monochromatic x-ray of wavelength λ, the complex amplitude of the transmitted wave in the object plane immediately behind the object is assumed to be composed of two components: an intense illuminating field $b(u,v)$, and a weak scattered field $f(u,v)$, which is of finite extent $\sigma_u \times \sigma_v$, generated by the object. In the far-field plane at a distance of z downstream of the object plane, an array filter is inserted to make an intensity measurement for the phase retrieval. We assume that the filter consists of $N \times M$ square apertures of each width w distributed over a Cartesian grid of period d. Then the filled apertures at the center of the array filter are utilized as a beam stop. In this subsection, we suppose that there is not a beam stop on the array filter (i.e., the filled apertures shown in Fig. 1 are opened).

Under the Fraunhofer approximation [14] for the diffraction from the object, the complex amplitude of the incident light to the array filter is given by

$$P(x,y) = \exp\left[i\frac{\pi}{\lambda z}(x^2+y^2) \right] \int\int_{-\infty}^{\infty} [b(u,v) + f(u,v)] \exp\left[-i\frac{2\pi}{\lambda z}(xu+yv) \right] du dv . \quad (1)$$

Then, using the Fresnel approximation [14], we can obtain the amplitude distribution in the detector plane at a distance of l downstream from the array filter as

$$G(\xi,\eta) = \int\int_{-\infty}^{\infty} P(x,y)\, A(x,y) \exp\left\{ i\frac{\pi}{\lambda l}[(x-\xi)^2 + (y-\eta)^2] \right\} dx dy, \quad (2)$$

where $A(x, y)$ is the function of an aperture-array filter:

$$A(x, y) = \sum_{n=-N/2}^{N/2-1} \sum_{m=-M/2}^{M/2-1} R(x - x_n, y - y_m) \ , \tag{3}$$

in which $R(x - x_n, y - y_n)$ denotes the amplitude transmittance of a square aperture being at the position of the coordinates $(x_n, y_m) = (nd, md)$ [$R(x, y) = 1.0$ for $-w/2 \le x \le w/2$, $-w/2 \le y \le w/2$ and $R(x, y) = 0$ otherwise]. In Eqs. (1) and (2), unimportant multiplicative constants associated with the diffraction integrals are ignored. We now rewrite Eq. (1) as

$$P(x, y) = \exp\left[i \frac{\pi}{\lambda z}(x^2 + y^2) \right] \left[B(x, y) + F(x, y) \right], \tag{4}$$

where $B(x, y)$ and $F(x, y)$ denote the Fourier transforms of $b(u, v)$ and $f(u, v)$, respectively. After substituting Eq. (4) into Eq. (2), the two quadratic phase terms are combined into one term, and then Eq. (2) becomes

$$G(\xi, \eta) = \int\int_{-\infty}^{\infty} \left[B(x, y) + F(x, y) \right] A(x, y) \times \exp\left\{ i \frac{\pi\alpha}{\lambda l} \left[\left(x - \frac{\xi}{\alpha} \right)^2 + \left(y - \frac{\eta}{\alpha} \right)^2 + \frac{l\left(\xi^2 + \eta^2\right)}{z\alpha^2} \right] \right\} dxdy, \tag{5}$$

where $\alpha = 1 + l/z$. As described in the previous paper [12], the diffraction pattern of each aperture in the detector plane is isolated approximately from those of the adjoining square if the parameters of the measurement system (i.e., $z, l, w,$ and, d) satisfy a condition $d(1 + l/z) > \varepsilon(2\lambda l / w + l\sigma_j / z)$ $(j = u, v)$, where $d(1 + l/z)$ denotes the period of the Fresnel diffraction pattern of the array in the detector plane, $2\lambda l / w + l\sigma_j / z$ (in which σ_j is the extent of the object function in the direction of u or v) represents the main width of the diffraction pattern of each square aperture in the case of the far-field diffraction, and ε indicates a compensation parameter for increase of the main width in the case of the Fresnel diffraction.

Then the increase of the main width can be roughly calculated from the rough extent of the object and the Fresnel diffraction pattern of the aperture function. This condition determines only the parameters for the use of the phase retrieval, and then it does not restrict the applicability of the interpolation method for the missing data in Subsection 2.B. Under that condition, the observable intensity of Eq. (5) at the discrete coordinates $\xi_n = \alpha x_n$ and $\eta_m = \alpha y_m$ $(n = -N/2 \cdots, 0, \cdots N/2-1,$ and, $m = -M/2 \cdots, 0, \cdots M/2-1)$ can be represented by

$$\left|G(\alpha x_n, \alpha y_m)\right|^2 = \left| \int\int_{-\infty}^{\infty} \left[B(x,y) + F(x,y)\right] R'(x - x_n, y - y_m) dxdy \right|^2, \tag{6}$$

where $R'(x,y)$ is the aperture function including the quadratic phase:

$$R'(x,y) = R(x,y) \exp\left[i \frac{\pi\alpha}{\lambda l} (x^2 + y^2) \right]. \tag{7}$$

Since the Fourier intensity $\left|F(x,y)\right|^2$ of the object function $f(u,v)$ has to be encoded into the discrete data of Eq. (6), we here assume that the extent of the array filter (i.e., $dN \times dM$) is sufficiently large to enable a satisfactory representation of the object, and that the period d of the array fulfills the condition of $d \le \lambda z / 2\sigma_j$ ($j = u, v$). As described in the previous paper [12], the 1-D phases in the direction of ξ and η axes of the correlation integral in Eq. (6) can be retrieved from the intensity distributions $\left|G(\alpha x_n \pm \tau, \alpha y_m)\right|^2$ and $\left|G(\alpha x_n, \alpha y_m \pm \tau)\right|^2$, respectively, with several values of τ (where τ is a known constant), which correspond to the multiple groups of sampling data of a single intensity distribution $\left|G(\xi,\eta)\right|^2$ of Eq. (5). Then the 2-D phase of the correlation integral can be obtained by combining those 1-D phases in the direction

of ξ and η axes. Using the same way as in Eqs. (5) and (6), we can obtain the intensity $\left|G(\alpha x_n \pm \tau, \alpha y_m)\right|^2$:

$$\left|G(\alpha x_n \pm \tau, \alpha y_m)\right|^2 = \left| \int\int_{-\infty}^{\infty} [B(x,y) + F(x,y)] R'(x - x_n, y - y_m) \exp\left(\mp i \frac{2\pi}{\lambda l} x\tau \right) dxdy \right|^2, \quad (8)$$

and also $\left|G(\alpha x_n, \alpha y_m \pm \tau)\right|^2$ is given by substituting $\exp\left(\mp i 2\pi y\tau / \lambda l\right)$ into Eq. (8) instead of $\exp\left(\mp i 2\pi x\tau / \lambda l\right)$.

In measuring a diffraction pattern, the central intensities of the object's scattered field $F(x,y)$ overlap with the intense direct beam $B(x,y)$, and so are blocked by a beam stop. Since the central intensities of $F(x,y)$ correspond to the lower spatial frequency of the object structure, their absence makes the phase retrieval impossible. In the following subsection, we present the application of a noniterative interpolation method to the recovery of the missing data.

B. Interpolation Method Based on the Sampling Theorem

In the present method, some filled apertures on the array filter are utilized as a beam stop. Then the beam stop is assumed to have the extent of $[(2n_c + 2)d - w] \times [(2m_c + 2)d - w]$ and to be symmetrical with respect to the origin (i.e., $n_c = m_c$), in which n_c (or m_c) is the number of apertures from the central aperture at the position of the coordinates $(x_0, y_0) = (0,0)$ in the positive direction of x (or y) axis. In addition, we assume that all energies of the waves, including the intense direct beam $B(x,y)$ and the lower spatial-frequency components of the object's field $F(x,y)$, are blocked by the beam stop. Thus, a 1-D interpolation method based on the sampling theorem [13] is applied to estimate the missing data of $F(x,y)$ as follows.

For aperture indices (n,m) within the area of the beam stop, we make no measurements of the intensity functions $|G(\alpha x_n, \alpha y_m)|^2$ given by Eq. (6) since these apertures are blocked. On the other hand, for aperture indices (n,m) outside of the beam stop, we do measure the corresponding functions $|G(\alpha x_n, \alpha y_m)|^2$, and then the area of the measurements are beyond the region of support for the direct beam $B(x,y)$. Therefore we can simplify Eq. (6) by setting $B(x,y)$ equal to zero. Thus, the observable diffraction intensities in the detector plane are given by

$$|G(\alpha x_n, \alpha y_m)|^2 = \left| \int\int_{-\infty}^{\infty} F(x,y) R'(x - x_n, y - y_m) dx dy \right|^2 . \tag{9}$$

Then the inverse Fourier transform of Eq. (9) is written as

$$\Im^{-1}\left[|G(\alpha x_n, \alpha y_m)|^2 \right] = g(u,v) \square\ g(u,v), \tag{10}$$

where $\Im^{-1}$ denotes the inverse Fourier transform, the symbol $\square$ indicates the autocorrelation operation, and the function $g(u,v)$ is given by

$$g(u,v) = f(u,v)\, r'(u,v), \tag{11}$$

in which $r'(u,v)$ denotes the inverse Fourier transform of the aperture function $R'(x,y)$ in Eq. (7). The extent of $r'(u,v)$ is larger than the object's extent, because the width w of the aperture function $R'(x,y)$ is smaller than the period $d\ (\leq \lambda z / 2\sigma_j,\ j = u,v)$ of the array filter. Thus the extent of the function $g(u,v)$ is determined by the extent $\sigma_u \times \sigma_v$ of the object function $f(u,v)$. Therefore the autocorrelation function of Eq. (10) is a band-limited function with the extent $2\sigma_u \times 2\sigma_v$. By the Whittaker-Shannon sampling theorem, the 1-D intensity distribution of Eq. (9) on the coordinates ($\xi_n = \alpha x_n$) along a line parallel to the ξ axis can be written in terms of its sample values at frequencies k / L :

$$\left|G(\alpha x_n, C)\right|^2 \cong \sum_{k=-K/2}^{K/2-1} \left|G\left(\frac{\alpha k}{L}, C\right)\right|^2 \operatorname{sinc}\left[L\left(x_n - \frac{k}{L}\right)\right], \tag{12}$$

where $\operatorname{sinc}(x) = \sin(\pi x)/(\pi x)$, $L = 2\sigma_u$, and $C = \alpha y_{m'}$, in which the numerical subscript m' is set to be a constant within $-m_c \le m' \le m_c$. To determine the $2n_c + 1$ missing data of $\left|G(\alpha x_n, C)\right|^2$ in Eq. (9) within the extent of the beam stop, we have to measure the values of $\left|G(\alpha k/L, C)\right|^2$ at any K distinct frequencies k/L, where the integer value K is chosen for $K/L \le (Nd/\lambda z) < (K+1)/L$. The k/L in general will not coincide with the aperture's position x_n. Thus, when the condition $N - K \ge 2n_c + 1$ [i.e., $N - Nd/(\lambda z/L) \ge (2n_c + 1)$] is satisfied in the measurement system, the values of $\left|G(\alpha k/L, C)\right|^2$ are determined from the observable data $\left|G(\alpha x_n, C)\right|^2$ in the area excluding the extent of the beam stop by solving a set of K linear equations of the form

$$\left|G(\alpha x_n, C)\right|^2 = \sum_{k=-K/2}^{K/2-1} \left|G\left(\frac{\alpha k}{L}, C\right)\right|^2 \operatorname{sinc}\left[L\left(x_n - \frac{k}{L}\right)\right] \quad n = -\frac{K+2n_c}{2}, \cdots, -n_c - 1,\ n_c + 1, \cdots, \frac{K+2n_c}{2}. \tag{13}$$

Hence the $2n_c + 1$ missing data of $\left|G(\alpha x_n, C)\right|^2$ within the extent of the beam stop can be calculated by substituting the values of $\left|G(\alpha k/L, C)\right|^2$ into Eq. (12). Using the same way as in Eqs. (9)-(13), the missing data of $\left|G(\alpha x_n \pm \tau, C)\right|^2$ or $\left|G(C', \alpha y_m \pm \tau)\right|^2$ (in which $C' = \alpha x_{n'}$ is a constant within $-n_c \le n' \le n_c$) can be determined from intensity data $\left|G(\alpha x_n \pm \tau, C)\right|^2$ or $\left|G(C', \alpha y_m \pm \tau)\right|^2$ in the area excluding the extent of the beam stop. Note that, if the condition $N - Nd/(\lambda z/L) \ge (2n_c + 1)$ is not satisfied, the $2n_c + 1$ missing data cannot be obtained from observable intensities by solving the linear equations in Eq. (13). Therefore we have to set the

interval d of the aperture array to be not exceeding of up to $\left[1-(2n_c+1)/N\right](\lambda z/L)$. In Section 3, we will discuss the stability of linear equations for specific examples in computer simulations.

By using the method in the previous paper [12], the 1-D phases on the coordinates αx_n and αy_m along the lines parallel to the ξ and η axes, respectively, are retrieved from the intensity distributions $\left|G(\alpha x_n \pm \tau, C)\right|^2$ and $\left|G(C', \alpha y_m \pm \tau)\right|^2$ with the interpolated data, and then the 2-D phase of the convolution integral in Eq. (9) is obtained by combining those 1-D phases. Since the inverse Fourier transform of that convolution integral corresponds to the function $g(u,v)$ in Eq. (11), the object function $f(u,v)$ can be reconstructed through compensation for the known function $r'(u,v)$. Note that, although it is possible to do the 2-D interpolation calculation from the intensity data of $\left|G(\alpha x_n, \alpha y_m)\right|^2$ excluding the beam stop's area, the 1-D interpolation method is not so time-consuming as the 2-D one and is suitable for the present method based on the 1-D phase retrieval. In the next section, the usefulness of the phase retrieval with the 1-D interpolation method is presented in the computer simulations.

3. COMPUTER SIMULATIONS

The performance of the interpolation method for missing data on phase retrieval is demonstrated by computer simulations. Figures 2 and 3 show an example of the object reconstruction using that method. Figures 2(a) and 2(b) show the modulus and the phase of the original object function, where the figures are represented by 64×64 points. Data processing for calculating the diffraction integral by means of a fast Fourier transform was carried out with 2048×2048

sampling points, of which the central part (64×64 points) is shown in Figs. 2(a) and 2(b). The physical size of the object, shown in the central area (27×27 points) of the figures, is assigned to $\sigma_u \times \sigma_v = 0.844\times0.844\,\mu$m. The phase distribution in Fig. 2(b) is in the range of from -2.05 to 1.16 rad. We assume that the object is illuminated by a monochromatic x-ray with wavelength 1nm. The distance between the object and the far-field planes is set to $z = 80\,$mm. The aperture-array filter in the far-field plane is assumed to be a uniform square grid of interval $d = 40\,\mu$m with 64×64 square apertures each of width $w = 10\,\mu$m, and the distance between the filter and the detector planes is set to be $l = 400\,$mm. These parameters for the simulation are satisfied with the sufficient condition for the isolation of the diffraction patterns from the apertures of the filter, which was described in Subsection 2.A. Figure 2(c) shows the intensity distribution in the detector plane, which is represented on a base-10 logarithmic gray scale of a normalized intensity truncated to 10^{-3} for display purposes. In the simulations of Figs. 2 and 3, 3×3 square apertures around the center of the filter were closed, which corresponds to a beam stop with the extent $[(2n_c+2)d-w]\times[(2m_c+2)d-w]$ for $n_c = m_c = 1$, and the direct beam $B(x,y)$ in Eq. (4) is assumed to be entirely blocked by the beam stop [i.e., $B(x,y)\equiv0$]. Figures 3(a) and 3(b) [or 3(c) and 3(d)] show the modulus and the phase, respectively, of the reconstructed object from noiseless intensity data of Fig. 2(c) without (or with) the interpolation for the missing data. Then the calculation of phase retrieval for Figs. 3(a) and 3(b) [or 3(c) and 3(d)] was carried out from the intensity distributions at the coordinates (ξ_n,η_m), $(\xi_n\pm\tau,\eta_m)$, and $(\xi_n,\eta_m\pm\tau)$ in the detector plane, not including [or including] the interpolated data, where twenty values of τ at 1.25μm spacing in a range of $0<\tau<25\mu$m were utilized to improve the accuracy of the phase calculation according to the procedure in the previous paper [12]. Since those coordinates did

not coincide with the positions of the uniformly sampled data (2048×2048 points with 7.5μm spacing) of the intensity in the detector plane, the intensity data at those coordinates were calculated from the uniformly sampled intensity data by linear interpolation. In Figs. 3(c) and 3(d), the missing data on each of the 1-D lines passing through the area of the beam stop were interpolated by substituting the solution of a set of $61[=N-(2n_c+1)]$ linear equations in Eq. (13) into Eq. (12). For the stability of the solution of the linear equations, the condition $N-Nd/(\lambda z/L)\geq(2n_c+1)$ has to be satisfied, where $L=2\sigma_j$ ($j=u,v$) is the extent of the autocorrelation function of the object in the direction of u or v. The value of $N-Nd/(\lambda z/L)$ for Figs. 2 and 3 becomes about 9.98, which fulfills that condition. For comparison, a reconstructed object from an intensity distribution obtained without both the beam stop and the direct beam is shown in Figs. 3(e) and 3(f).

To evaluate the difference between an original and a reconstructed object, a measure of the quality of reconstruction is defined by the normalized root-mean-square (NRMS) error,

$$\mathrm{ER}=\left[\frac{\sum_{u,v\in\sigma}\left|f(u,v)-f_r(u,v)\right|^2}{\sum_{u,v\in\sigma}\left|f(u,v)\right|^2}\right]^{1/2}, \tag{14}$$

where $f(u,v)$ and $f_r(u,v)$ are the original and the reconstructed object functions, respectively, at the 2-D coordinates u and v, and σ denotes the extent of $f(u,v)$. Then the NRMS errors for the reconstructed objects in Figs. 3(a) and 3(b), 3(c) and 3(d), and 3(e) and 3(f) are 0.796, 0.241 and 0.229, respectively. It can be seen from Figs. 3(c) and 3(d), and, 3(e) and 3(f) that the reconstruction with the interpolation method for the missing data is almost as good as that from the intensity measurement without both the beam stop and the direct beam. The remaining errors

in Figs. 3(c) and 3(d) [or 3(e) and 3(f)] are due mainly to the systematic errors in the data such as errors in interpolation and aliasing in discrete Fourier transforms for the object with the finite extent.

In calculating the solution of the linear equations in Eq. (13), it is necessary to know the extent of the autocorrelation function of the object [i.e., $L = 2\sigma_j$ ($j = u, v$)] as precisely as possible. Since the extent L is estimated practically from the inverse Fourier transform of the observable data $\left|G(\alpha x_n, \alpha y_m)\right|^2$ excluding the area of the beam stop, some errors of the estimation arose. Thus, as shown in Fig. 4, we investigated the dependence of the NRMS error for the object reconstruction on the normalized deviations $L/2\sigma_j$ from the true extent $2\sigma_j$ ($j = u, v$), where the same deviation was used in the directions of u and v. In the simulations of Fig. 4, the same object function and parameters as in Figs. 2 and 3 were used except for changes of the extent L in Eqs. (12) and (13) and the number of filled apertures on the array filter. In Fig. 4, the open circles and squares indicate the NRMS errors as a function of $L/2\sigma_j$ for 3×3 and 5×5 filled apertures, respectively, around the center of the array filter. The estimation of the missing data failed in the cases of $L/2\sigma_j = 1.1$ and over for 5×5 filled apertures (or $L/2\sigma_j = 1.15$ and over for 3×3 filled ones), because the stability condition $N - Nd/(\lambda z / L) \geq (2n_c + 1)$ for the solution of the linear equations becomes to be not satisfied in these cases. Figure 4 shows that it is allowable to underestimate the extent L until about 30% of the true extent. This is because the autocorrelation function of an object with a finite extent σ has dully decreasing amplitude in the vicinity of the boundary of its extent 2σ.

When the number of filled apertures is 7×7 or more, the present interpolation method cannot reconstruct the missing data reliably. On the other hand, it has been shown in the

iterative approach to the missing data problem [8] that the iterative phase-retrieval method yields a reliable reconstruction from the intensity distribution with the central missing part when the missing data are confined within a central speckle size which is proportional to the inverse of the object extent (i.e., when the number of the missing speckles, defined by Eq. (1) in [8], is less than one). The number of the missing speckles is calculated from the number of missing data and a ratio of the spatial frequency $\lambda z/\sigma_j$ ($j = u, v$) to the sampling interval d (i.e., an oversampling ratio). In order to compare the present method with the iterative method, we evaluate the number of missing speckles for the present examles. Then the number of missing speckles for the cases of 3×3, 5×5, and 7×7 filled apertures in the present simulations become 0.422, 0.844, and 1.27, respectively. Therefore, it is found that the present phase retrieval method with the noniterative interpolation gives the reliable solution to the missing data problem under almost the same condition as that in the iterative method.

To simulate the object reconstruction in more practical cases, an intense direct beam is added to the object's wave in the object plane, and noises are added to the intensity distribution in the detector plane. For simplicity, the intense direct beam $b(u,v)$ is assumed to be a Gaussian function $a\exp\left[-4(u^2+v^2)/\delta_b{}^2\right]$, where a and δ_b are the central value and the full-width at 1/e maximum of the function, respectively. The extent of the direct beam which can be blocked by a beam stop is depended on the central value a of the direct beam. From computer simulations, it was found that, if the extent δ_b of the direct beam is at least four times wider than the object's extent σ_j ($j = u, v$), the beam stop of 3×3 filled apertures can block the direct beam of the central value a that is even ten thousand times larger than the maximum value of the object modulus. Thus, Figure 5 shows the reconstruction with the same object and parameters as in

Figs. 2 and 3 in the case that the extent δ_b and the central value a of the direct beam are set to $4\sigma_j$ ($j = u, v$) and ten thousand times larger value than the maximum object's modulus, respectively. Figure 5(a) shows the modulus of the wave field immediately in front of the array filter [i.e., $P(x, y)$ in Eq. (1)], which is represented on a base-10 logarithmic gray scale of a normalized modulus truncated to 10^{-5} for display purposes. To simulate the effect of noise on the reconstructed object, Gaussian random noises with a zero mean and a standard deviation were produced by a computer and were added to the observable modulus $|G(\xi,\eta)|$ in the form $|G_n(\xi,\eta)| = ||G(\xi,\eta)| + n(\xi,\eta)|$. A factor of the signal-to-noise ratio (SNR) is defined by the ratio of the total intensities for the modulus data and the noises in the detector plane [i.e., $\mathrm{SNR} = \sum_{\xi,\eta}|G(\xi,\eta)|^2 \Big/ \sum_{\xi,\eta}|n(\xi,\eta)|^2$]. To reduce the effect of noises on the solution of a linear equation in Eq. (13), the observable intensities on the left-hand side of Eq. (13) were multiplied by a 1-D Gaussian function as a weighting function that can be used to emphasize regions with high SNR around the missing data area, and then the intensities retrieved by substituting the solution of Eq. (13) into Eq. (12) were compensated for by multiplying by the inverse function of the 1-D Gaussian function.

Figure 5(b) and 5(c) [or 5(d) and 5(e)] show the modulus and the phase, respectively, of the reconstructed object from noisy data for SNR=184 (or SNR=46) with the interpolation of the missing data, where the corresponding standard deviation of the Gaussian random noises is 1/2.63 (or 1/1.32) of the average value of the observable modulus in the detector plane. Note that the SNR=184 and SNR=46 correspond to 22.6 and 16.6 decibels (dB), respectively. Then the NRMS errors for the reconstructed objects in Figs. 5(b) and 5(c), and, 5(d) and 5(e) are 0.255 and 0.277, respectively. On the other hand, the object reconstruction with the beam stop of 5×5

filled apertures did not yield reliable results when the SNR was lower than about one thousand. Consequently, the condition for applying the present interpolation method to the cases with a practical level of noise is that the number of the missing speckles needs to be less than about 0.5, which is evaluated by substituting the number of missing points $2n_c+1=3$ and the minimum oversampling ration 2.0 for phase retrieval into the defined equation in [8].

4. Conclusions

We have presented the combined use of the noniterative phase retrieval method using an aperture-array filter [12] and the interpolation method based on the sampling theorem for the object reconstruction from a diffraction intensity with the missing data due to a beam stop. Since the phase of the diffracted wave from an object is retrieved from multiple groups of sampling data of a single intensity distribution in the detector plane by the noniterative phase retrieval method, the missing data for each of the multiple groups of sampling data have to be estimated by the interpolation method. In that case, the use of the present interpolation method based on the 1-D sampling theorem is not so time-consuming as the use of the iterative interpolation algorithm or the 2-D version of the 1-D interpolation method, and also is suitable for the noniterative phase retrieval based on the 1-D calculations along lines on the 2-D plane.

We have demonstrated in computer simulations that the present method can cope with the reconstruction of a complex-amplitude object, which is generally difficult to treat with the iterative method because a nonnegativity constraint cannot be used. The present method

yields the reliable reconstruction of an object from a diffraction intensity pattern when the number of missing speckles in this intensity pattern is less than one. This condition of the missing speckles in the present method is almost the same as that in the iterative phase-retrieval method [8]. However, it was also shown that the number of missing speckles should be less than 0.5 in order to reconstruct the object reliably at a practical level of noise. In particular, we have demonstrated that, even if the central value of an intense direct beam with a Gaussian modulus is ten thousand times larger than the maximum value of the object's modulus, the object can be reliably reconstructed from the far-field diffraction intensity with the missing data (in which the number of missing speckles is 0.422), provided that the extent of the intense direct beam is at least four times larger than that of the object.

In practical cases, we need to know the extent of the autocorrelation function of an object for the solution to the missing data problem. Since the stable performance of the present method has been verified by computer simulations despite the poor tolerance for the estimation of the extent, it would be possible to use the estimated extent from the inverse Fourier transform of the diffraction intensity with the missing data. Consequently, we will be able to use the present method for the coherent diffraction imaging with the missing area due to a beam stop, for example, ultrafast single-shot imaging with x-ray free-electron lasers [15].

Acknowledgements

This research was supported by a Grant-in-Aid for Scientific Research from Japan Society for the Promotion of Science.

References

1. J. Miao, P. Charalambous, J. Kirz, and D. Sayre, "Extending the methodology of X-ray crystallography to allow imaging of micrometre-sized non-crystalline speciments," Nature **400**, 342-344 (1999).
2. J. Miao, T. Ishikawa, B. Johnson, E. H. Anderson, B. Lai, and K. O. Hodgson, "High resolution 3D x-ray diffraction microscopy," Phys. Rev. Lett. **89**, 088303 (2002).
3. S. Marchesini, H. He, H N. Chapman, S. P. Hau-Riege, A. Noy, M R. Howells, U. Weierstrall, and J. C. H. Spence, "X-ray image reconstruction from a diffraction patter alone," Phys. Rev. B **68**, 140101(R) (2003).
4. H. N. Chapman, A. Barty, S. Marchesini, A. Noy, S. P. Hau-Riege, C. Cui, M. R. Howells, R. Rosen, H. He, J. C. H. Spence, U. Weierstall, T. Beetz, C. Jacobsen, and D. Shapiro, "High-resolution *ab initio* three-dimensional x-ray diffraction microscopy," J. Opt. Soc. Am. A **23**, 1179-1200 (2006).
5. I. K.Robinson, I. A. Vartanyants, G. J. Williams, M. A. Pfeifer, and J. A. Pitney, "Reconstruction of the shapes of gold nanocrystals using coherent x-ray diffraction," Phys. Rev. Lett. **87**, 195505 (2001).
6. K. A. Nugent, A. G. Peele, H. N. Chapman, and A. P. Mancuso, "Unique phase recovery for nonperiodic objects," Phys. Rev. Lett. **91**, 203902 (2003).
7. J. Miao, P. Charalambous, J. Kirz, and D. Sayre, "Extending the methodology of X-ray crystallography to allow imaging of micrometre-sized non-crystalline speciments," Nature **400**, 342-344 (1999).

8. J. Miao, Y. Nishino, Y. Kohmura, B. Johnson, C. Song, S. H. Risbud, and T. Ishikawa, "Quantitative image reconstruction of GaN quantum dots from oversampled diffraction intensities alone," Phys. Rev. Lett. **95**, 085503 (2005).
9. J. R. Fienup, "Reconstruction of a complex-valued object from the modulus of its Fourier transform using a support constraint," J. Opt. Soc. Am. A **4**, 118-123 (1987).
10. J. R. Fienup, "Lensless coherent imaging by phase retrieval with an illumination pattern constraint," Opt. Express **14**, 498-508 (2006).
11. J. Miao, D. Sayre, and H. N. Chapman, "Phase retrieval from the magnitude of the Fourier transforms of nonperiodic objects," J. Opt. Soc. Am. A **15**, 1662-1669 (1998).
12. N. Nakajima, "Lensless coherent imaging by a deterministic phase retrieval method with an aperture-array filter," J. Opt. Soc. Am. A **25**,742-750 (2008).
13. J. L. Harris, "Diffraction and resolving power," J. Opt. Soc. Am. **54**, 931-936 (1964).
14. J. W. Goodman, *Introduction to Fourier Optics*, 2nd ed. (McGraw-Hill, New York, 1996), pp. 66-74.
15. R. Neutze, R. Wouts, D. van der Spoel, E. Weckert, and J. Hajdu, "Potential for biomolecular imaging with femtosecond x-ray pulses," Nature **406**, 752-757 (2000).

Figure Captions

Fig. 1. Schematic diagram of the measurement system. The filled apertures around the center of the array filter work as a beam stop that blocks the direct beam. The object function is reconstructed from a single intensity pattern of a diffracted wave through an array of square apertures by using the phase-retrieval method with the interpolation for the missing data due to the beam stop.

Fig. 2. Original object function used in the simulations: (a) modulus and (b) phase of an object with a rectangular extent of $0.844 \times 0.844\,\mu$m (where the values of the phase are in the range of −2.05 to 1.16 rad), and (c) intensity distribution in the detector plane of Fig. 1, where the central intensities are lost by a beam stop of 3×3 filled apertures and the direct beam is set to be zero. The only picture of (c) is represented on a base-10 logarithmic grey scale of a normalized intensity truncated to 10^{-3} for display purposes.

Fig. 3. Reconstruction of the object function shown in Fig. 2 from a noiseless intensity distribution in the detector plane: (a) and (b) [or (c) and (d)] are the modulus and phase, respectively, of a reconstructed object from the noiseless intensity in Fig. 2(c) without (or with) the interpolation for the missing data. (e) and (f) are the modulus and phase, respectively, of a reconstructed object from an intensity distribution obtained without both the beam stop and the direct beam.

Fig. 4. Dependence of the NRMS error (ER) on the normalized deviations $L/2\sigma_j$ from the true extent $2\sigma_j$ ($j = u, v$) of the autocorrelation of the object, where the same deviation in the directions of u and v is used at each coordinate. The circles and squares indicate the NRMS errors in the cases where 3×3 and 5×5 filled apertures, respectively, are used as a beam stop.

Fig. 5. Reconstruction of the object function shown in Fig. 2 from a noisy intensity distribution in the case where an intense direct beam with a Gaussian modulus is added to the object function: (a) modulus of the wave field immediately in front of the array filter with the beam stop of 3×3 filled apertures, which is represented on a base-10 logarithmic grey scale of a normalized modulus truncated to 10^{-5} for display purposes. (b) and (c) [or (d) and (e)] are the modulus and phase, respectively, of a reconstructed object from the noisy modulus for SNR=184 (22.6 dB) [or SNR=46 (16.6 dB)] with the interpolation for the missing data.

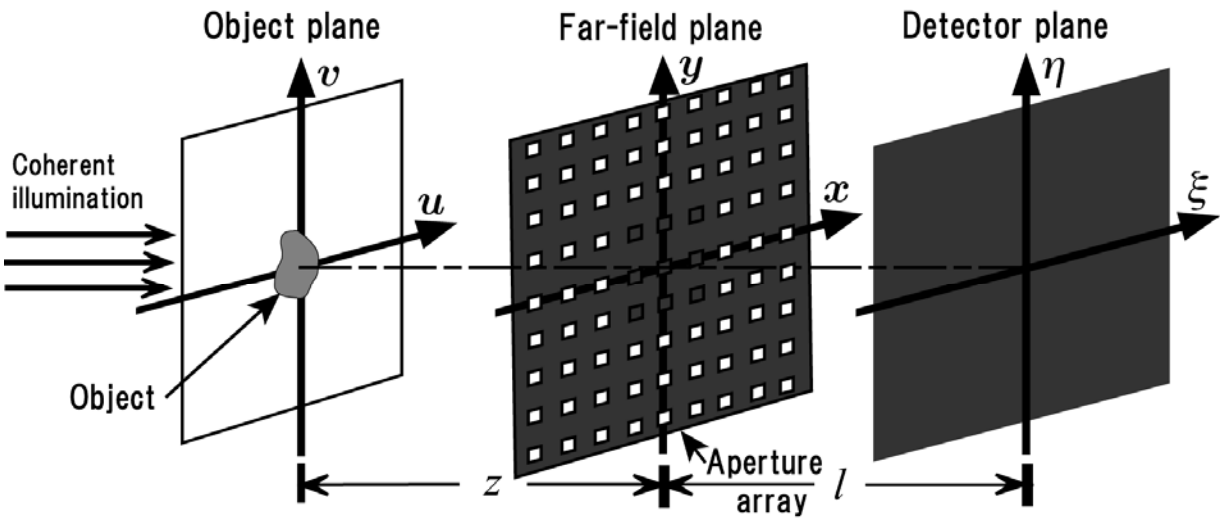
Object plane
Far-field plane
Detector plane
v
y
η
Coherent
illumination
u
x
ξ
Object
Aperture
array
z
l

Fig. 1

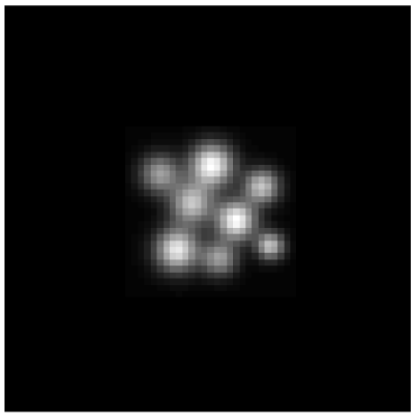

(a)

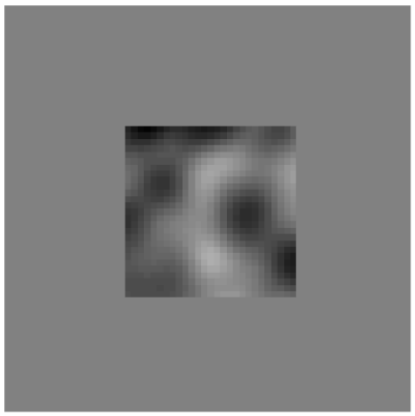

(b)

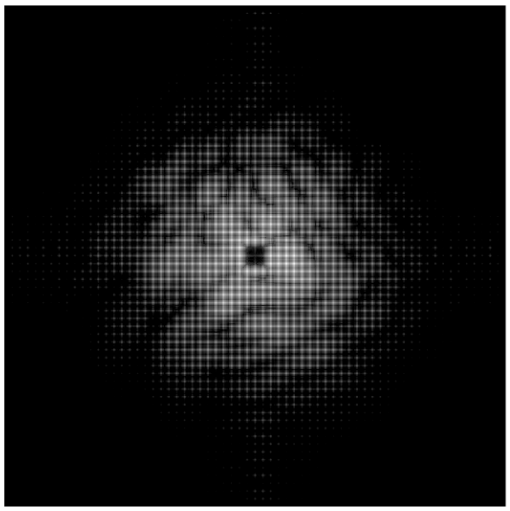

(c)

Fig. 2

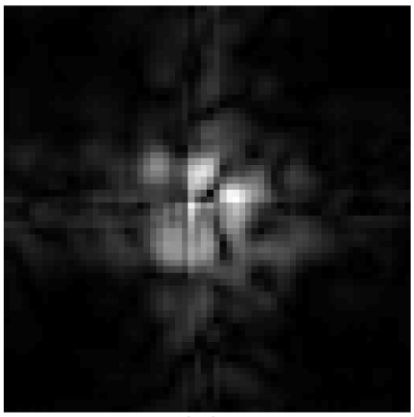

(a)

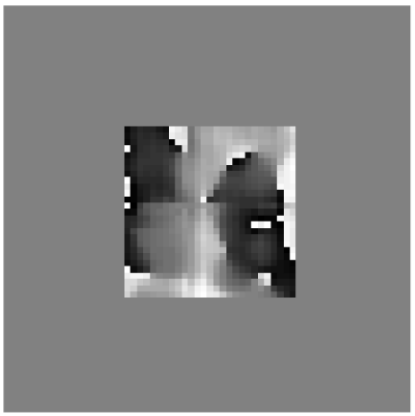

(b)

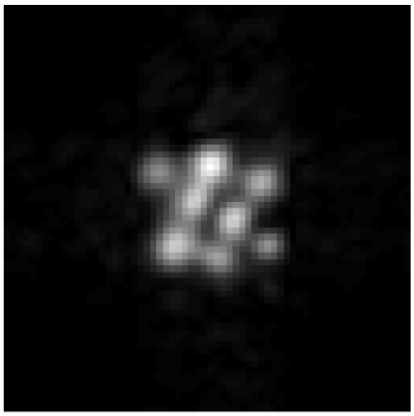

(c)

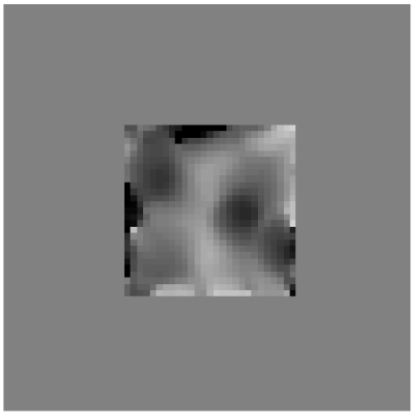

(d)

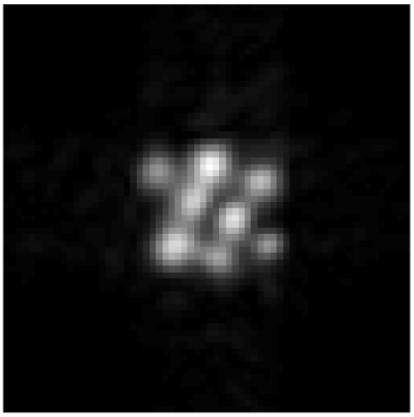

(e)

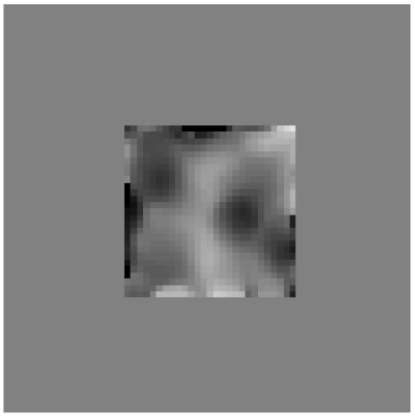

(f)

Fig. 3

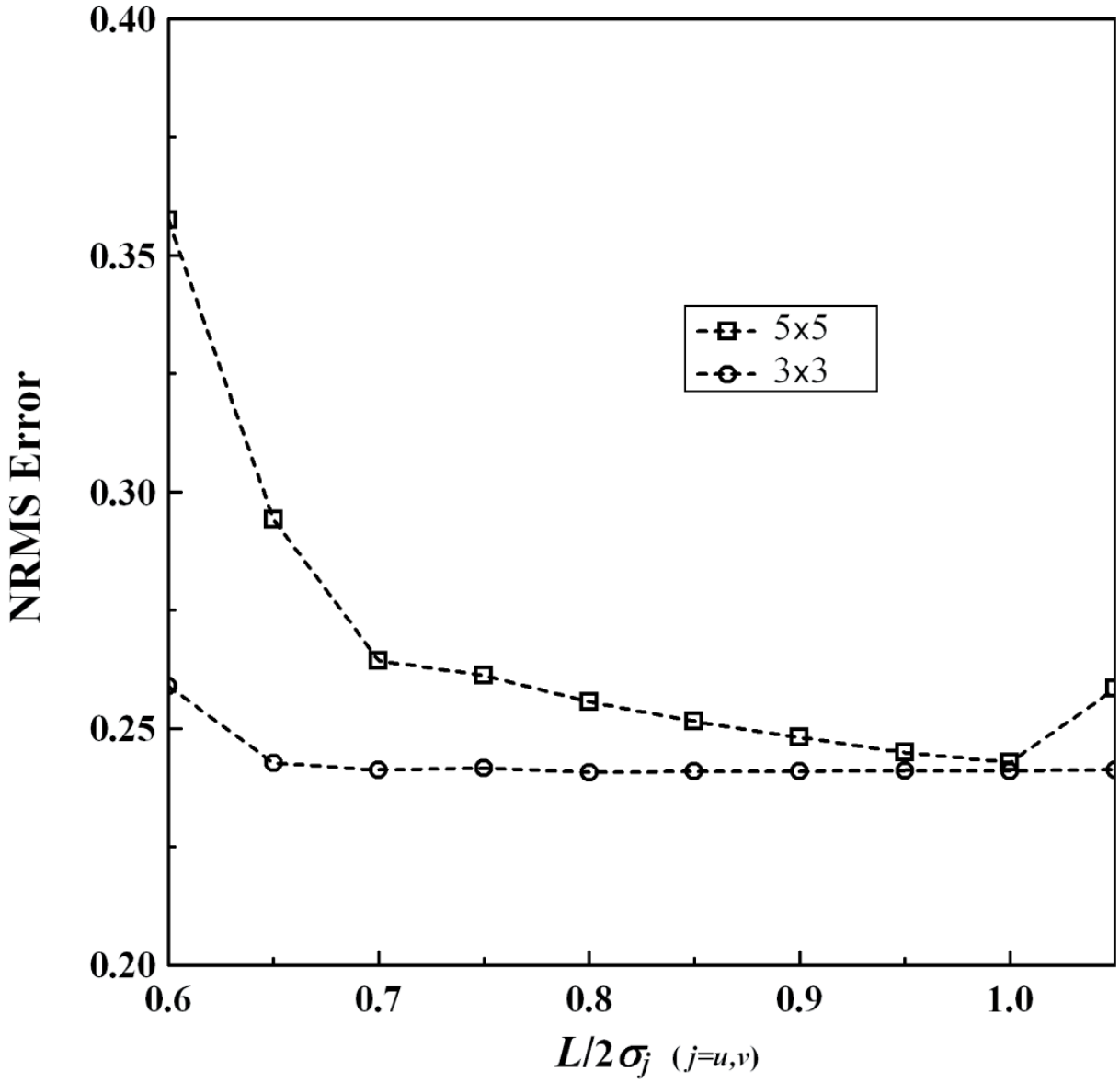

Fig. 4

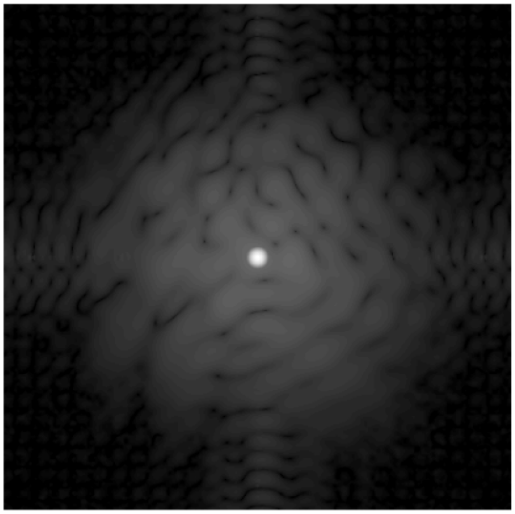

(a)

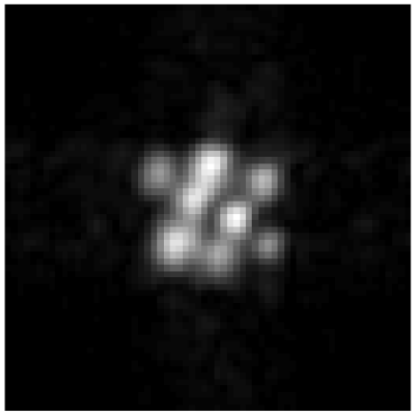

(b)

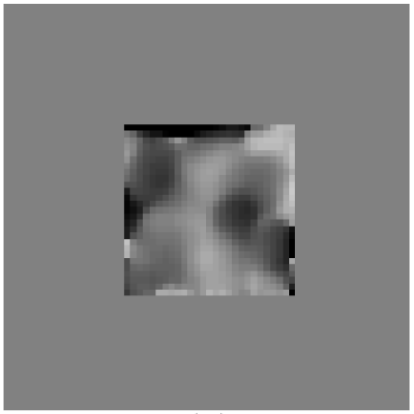

(c)

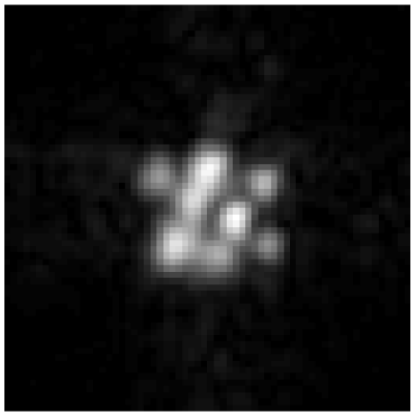

(d)

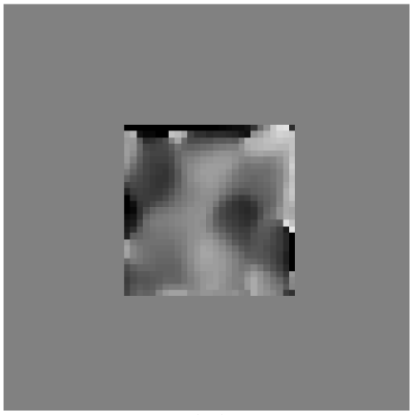

(e)

Fig. 5